Shehata, N., Meehan, K., Hudait, M., Jain, N., and Gaballah, S. (2014) Study of optical and structural characteristics of ceria nanoparticles doped with negative and positive association lanthanide elements. Journal of Nanomaterials, 2014 (401498). pp. 1-7. ISSN 1687-4110

Copyright © 2014 The Authors

http://eprints.gla.ac.uk/101003

Deposited on: 08 January 2015

Enlighten – Research publications by members of the University of Glasgow
http://eprints.gla.ac.uk

Hindawi Publishing Corporation
Journal of Nanomaterials
Volume 2014, Article ID 401498, 7 pages
http://dx.doi.org/10.1155/2014/401498

Research Article

Study of Optical and Structural Characteristics of Ceria Nanoparticles Doped with Negative and Positive Association Lanthanide Elements

N. Shehata,[1,2] K. Meehan,[3] M. Hudait,[1] N. Jain,[1] and S. Gaballah[2]

[1] *Bradley Department of Electrical and Computer Engineering, Virginia Polytechnic Institute and State University, Blacksburg, VA 24061, USA*
[2] *Department of Engineering Mathematics and Physics, Faculty of Engineering, Alexandria University, Alexandria 21544, Egypt*
[3] *School of Engineering, University of Glasgow, Glasgow G12 8QQ, UK*

Correspondence should be addressed to N. Shehata; nader83@vt.edu

Received 16 September 2014; Revised 5 November 2014; Accepted 8 November 2014; Published 30 November 2014

Academic Editor: Fathallah Karimzadeh

Copyright © 2014 N. Shehata et al. This is an open access article distributed under the Creative Commons Attribution License, which permits unrestricted use, distribution, and reproduction in any medium, provided the original work is properly cited.

This paper studies the effect of adding lanthanides with negative association energy, such as holmium and erbium, to ceria nanoparticles doped with positive association energy lanthanides, such as neodymium and samarium. That is what we called mixed doped ceria nanoparticles (MDC NPs). In MDC NPs of grain size range around 6 nm, it is proved qualitatively that the conversion rate from Ce^{4+} to Ce^{3+} is reduced, compared to ceria doped only with positive association energy lanthanides. There are many pieces of evidence which confirm the obtained conclusion. These indications are an increase in the allowed direct band gap which is calculated from the absorbance dispersion measurements, a decrease in the emitted fluorescence intensity, and an increase in the size of nanoparticles, which is measured using both techniques: transmission electron microscope (TEM) and X-ray diffractometer (XRD). That gives a novel conclusion that there are some trivalent dopants, such as holmium and erbium, which can suppress Ce^{3+} ionization states in ceria and consequently act as scavengers for active O-vacancies in MDC. This promising concept can develop applications which depend on the defects in ceria such as biomedicine, electronic devices, and gas sensors.

1. Introduction

In last few years, oxides with the cubic fluorite structure like cerium oxide (ceria) nanoparticles have been extensively studied due to their potential uses in various applications, such as UV absorbents [1], polishing media as luminescent material [2], neuroprotective applications [3], and catalysts in the fuel cell technology [4]. Doping ceria with trivalent elements changes the structural properties, compared to undoped ceria, such as decreasing in the lattice parameter which is caused by increasing the conversion process of Ce^{+4} ions to Ce^{3+} [5]. However, it is proved theoretically that few trivalent dopants such as scandia (Sc^{3+}), which has negative association energy between vacancy and dopant, can act as scavengers for oxygen vacancies (V_O) [6]. That may give an impression that perhaps not all trivalent doped elements increase the formation of oxygen vacancies in ceria nanoparticles. Many methods have been used to produce doped ceria nanoparticles such as chemical precipitation [7], hydrothermal synthesis [8], and solid-state reaction method [9]. Compared to other methods, precipitation is more attractive due to the cheap salt precursors, simple operation, and ease of mass production [10]. In this work, ceria nanoparticles are synthesized using chemical precipitation within two doping trivalent lanthanide elements; one has positive association energy (E_{ass}), such as neodymium and samarium, and the other one has negative association energy such as holmium and erbium [11, 12]. That is what we called mixed doped ceria nanoparticles (MDC NPs). The positive sign of E_{ass} indicates that the dopant can repel the O-vacancy or does not form complexes with oxygen vacancies, while the negative sign of E_{ass} means the dopant traps the O-vacancies [13]. There are some reported techniques to inspect conversion of Ce^{4+} ionization states to Ce^{3+} states, such as X-ray photoelectron

spectroscopy (XPS) and Raman spectroscopy [14, 15]. However, both techniques have significant drawbacks. In XPS, there is some ambiguity over the accuracy of the calculated ionization state of cerium because of an increase in the O-vacancy concentration observed under vacuum. Hence, this technique is not used to quantify the concentration of Ce^{4+} and Ce^{3+} in the nanoparticle samples [16]. Raman scattering is highly sensitive to laser instabilities, needs high resolution detection, and is subjected to saturation at the higher laser power density levels [17]. In the presented work, the experimental verifications used to prove the increase or decrease of O-vacancies in ceria, due to the selected lanthanide dopants compared to undoped ceria, are the direct allowed band gap, the amplitude of the fluorescence signal, grain size or average diameter, and lattice parameter. In this work, XPS is only used to analyze the chemical composition of the synthesized doped ceria nanoparticles to verify the molar fractions of the dopants. Raman spectroscopy was not performed as the environment of measurement has to be dry or slightly damp powders composed of the nanoparticles. In previous studies carried out in the lab, it was found that the Raman spectrum of the damp nanoparticles started to change after five minutes of exposure to air.

Within each prepared sample, some optical and structural characteristics are measured for the doped ceria nanoparticles. These optical characteristics are absorbance dispersion, direct allowed band gap, and emissive fluorescent intensity. The structural characteristics such as particle size and lattice parameter were measured through X-ray diffraction (XRD) pattern and nanoparticles imaging using transmission electron microscope (TEM). The measured characteristics of MDC NPs are compared to those of the doped ceria with only positive association energy elements to explain whether the added negative association energy lanthanide dopants decrease the conversion process between Ce^{4+} and Ce^{3+} or not. The control of oxygen vacancies in MDC NPs could have a positive impact on controlled high-κ ceria films deposited on germanium substrates to reduce the density of interface states in field effect transistor (FET) and consequently to reduce the leakage current [18]. In another field, the sensitivity and dynamic range of a ceria-based sensor can be controlled by optimizing the oxygen vacancy concentration in MDC [19]. Also, the control of oxygen vacancies can lead to improving the properties of ceria to act as free radical scavenger in biomedical applications [20].

2. Experimental Procedure

The doped ceria nanoparticles are prepared using chemical precipitation technique as synthesized by Chen and Chang [21] and Shehata et al. [22, 23] with some modifications. To prepare doped ceria with positive E_{ass}, 0.45 mg of cerium (III) chloride (heptahydrate, 99.9%, Aldrich Chemicals) and 0.05 mg of neodymium chloride (hexahydrate, 99.9%, Aldrich Chemicals) or samarium chloride (99.9%, Alfa Aesar) are initially added in 40 mL deionized (DI) water as a solvent. The solution is stirred at rate of 500 rpm for 24 hours through two stages. In the first stage, the stirring is started in a water path at 60°C and left for 1 minute, to ensure that the solution becomes homogenous. Then, 1.6 mL of ammonia is added. The heating stage is important because it helps in the conversion of $Ce(OH)_3$ to CeO_2; Ce^{4+} ions and then to Ce_2O_3; Ce^{3+} ions [24, 25]. However, the selected temperature is not relatively high, compared to [26, 27], to reduce the agglomeration of the formed nanoparticles. The stirred solution is kept in the heated water path for 1.5 hours. In the second stage of the stirring, the solution is stirred for the remaining 22.5 hours at room temperature. The long period of stirring leads to breaking any formed nanorods into nanoparticles. Then, the solution is centrifuged and washed with deionized water and ethanol twice to remove any unreacted cerium and ammonia. Between both centrifuging stages, the solution is sonicated to reduce the agglomeration probability of the formed ceria nanoparticles.

To synthesize MDC, the negative association energy lanthanides, Ho or Er, are doped using the previous procedure exactly, but holmium or erbium chlorides (both are hexahydrate, 99.9%, Aldrich Chemicals) are initially added to the previous precursors, including cerium and positive lanthanides chlorides. The weights of holmium and erbium chlorides are chosen once equal to the positive association chloride and, in another case, the negative association chlorides are double the weight of the positive association chlorides.

In both synthesized doped categories, doped ceria with only positive E_{ass} and MDC, the final centrifuged colloid is allowed to dry and 0.03 gm of the dried powder is sonicated in 10 mL of deionized water. This concentration is enough to get acceptable intensity peaks in the fluorescence spectroscopy. Approximately 3 mL of the colloidal solutions is pipetted into methacrylate cuvettes. The fluorescence spectroscopy system consists of xenon lamp coupled to a monochromator (a 1/4 m Newport Cornerstone 260). The light that exits the monochromator (λ_{exc} = 430 nm) is focused on the colloidal solution. The fluorescence signal is collected using a second monochromator (a 1/4 m Newport Cornerstone 260), positioned at a 90° angle to the first monochromator. Monochromator is scanned over the visible wavelength region and the fluorescence signal is detected by the photomultiplier tube (Newport PMT 77340), located at the exit port of the second monochromator, and is measured using a power meter (Newport Power meter 2935C).

To measure its absorbance dispersion, each solution is diluted 4 times, compared to the solution used in fluorescence spectroscopy, in a methacrylate cuvette and exposed to the light signal of the UV-Spectrometer, UV-3101PC, Shimadzu, with a reference light signal passing through another methacrylate cuvette filled with DI water. The allowed direct band gap is calculated from the linear region of the absorbance dispersion curves, as it will be discussed in Section 3.

To determine the structure of the doped and undoped nanoparticles, the surface planes of different samples are measured using a PANalytical X'Pert PRO X-ray diffractometer (XRD) at 45 KV and 40 A with Cu K_α radiation (λ = 0.154 nm). The average diameter of the nanoparticles can be

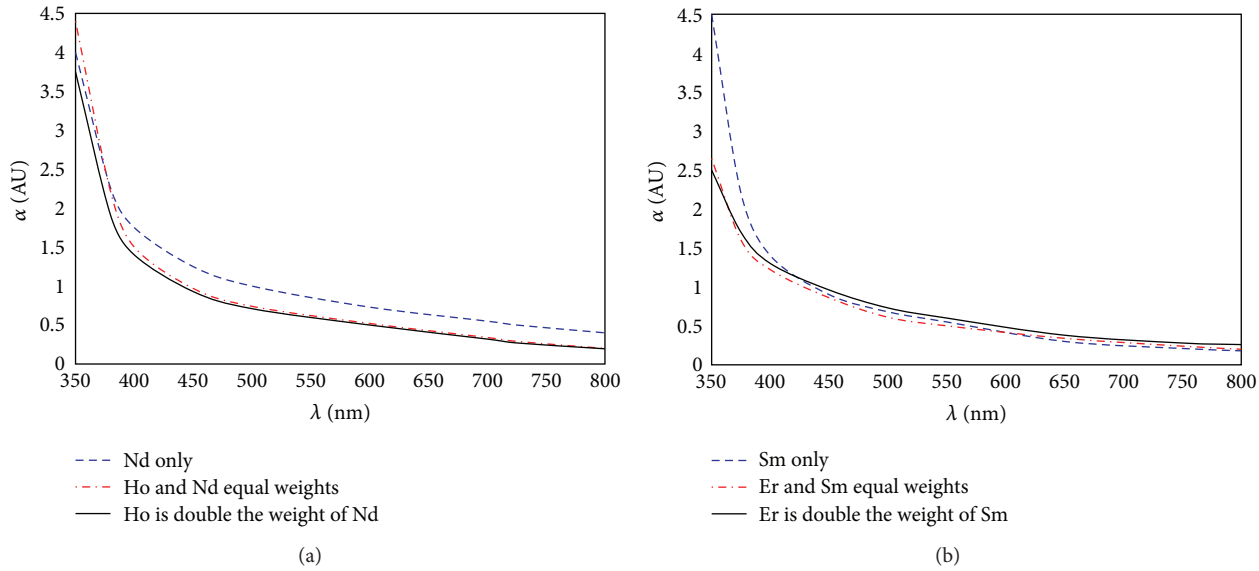

Figure 1: Absorbance dispersion of ceria, doped with (a) Nd and Ho and (b) Sm and Er.

calculated from the first diffraction peak, the plane (111) of ceria. Images of the doped and undoped nanoparticles of the different samples are collected using transmission electron microscopy (TEM) (Philips EM420). The TEM samples are prepared by immersing carbon-copper mesh grids in colloidal solutions with the same concentration of nanoparticles used during the absorption measurements; they are then left to be dried for 30 minutes before imaging. The average diameter of the nanoparticles is measured from the collected images and compared to the diameters calculated from XRD measurements. Also, the interplanar distance and the lattice parameter of the doped ceria nanoparticles can be calculated from the electron diffraction rings, which are obtained during TEM imaging.

The concentration of the chemical components of the synthesized nanoparticles is measured using a PHI Quantera SXM scanning X-ray photoelectron spectroscopy (XPS). Samples are prepared by drying colloidal solutions on quartz slides. Quantitative analyses of the chemical elements and their chemical states found within the top few nanometers of a surface are performed. Concentration of the dopant elements in the nanoparticles is determined from the XPS data given that there is some ambiguity over the accuracy of the calculated ionization state of cerium and this technique is not used to quantify the concentration of Ce^{4+} and Ce^{3+} in the nanoparticle samples [28], but it is used as a qualitative confirmation of the trends determined from an analysis of the data collected using the other characterization equipment.

3. Results and Discussion

The absorption coefficients of some MDC samples are measured over a wide range of wavelengths from 350 nm to 800 nm. As shown in Figure 1, the absorption dispersions for MDC, composed of different combinations of positive association lanthanides; Nd and Sm, with negative association elements; and Ho and Er are presented. For all samples, the absorbance dispersions have the shape, monotonically increasing with increasing photon energy, though there is slight difference in the magnitude and slope of the curves in the linear regions and the photon energy at which the nanoparticles begin to strongly absorb photons. Equation (1) shows the relation between the absorption coefficient and the absorbed photon energy [29]:

$$\alpha E = A\left(E - E_g\right)^{1/2}, \tag{1}$$

where α is the absorbance coefficient, A is a constant depending on the effective masses of electrons and holes of the material, E is the absorbed photon energy, and E_g is the direct allowed band gap.

From the resulting measurements of the linear region of the absorption dispersion curves, the curves of $(\alpha E)^2$ versus E are plotted in Figure 2 for some studied MDC samples. The extrapolation of the linear regions with E-axis gives the value of the allowed direct band gap. The complete measured data for all MDC NPs are presented in Table 1. From the semiconductors perspective, the band gap of CeO_2 is roughly 4 eV; however, Ce^{3+} ions presented in the crystal lattice, which could be considered a part of a Ce_2O_3 compound, create a trap state 3 eV above the CeO_2 valence band and correspond to the Ce5d–Ce4f transition [30]. Experimentally, the measured range of Ce_2O_3 band gap depends on the synthesis method, the used temperature, and the size of particles. Then, from our results, we could conclude that if the used dopants reduce the band gap of the doped ceria close to 3 eV, then there are more Ce^{3+} states formed. However, the value of band gap for the MDC becomes farther than 3 eV and hence the states of Ce^{3+} and the associated O-vacancies become less or suppressed, which is in agreement with similar trend presented in [22, 31].

Table 1: The complete measured data for MDC nanoparticles.

The used dopants within ceria	Direct Eg (eV)	Peak fluorescent intensity (arb. units)	Lattice parameter (nm)	Interplanar distance (nm)	Mean particle size using TEM (nm)	Mean particle size using XRD (nm)
Nd						
With no Ho or Er	3.22	37.90	0.535	0.309	6.39	6.45
With equal amount of Ho	3.26	22.11	0.514	0.297	6.48	6.56
With double amount of Ho	3.29	17.61	0.505	0.292	6.72	6.83
With equal amount of Er	3.27	20.47	0.532	0.307	6.60	6.55
With double amount of Er	3.28	15.92	0.528	0.305	6.69	6.83
Sm						
With no Ho or Er	3.23	33.95	0.531	0.307	6.23	6.29
With equal amount of Ho	3.29	23.09	0.514	0.297	6.39	6.30
With double amount of Ho	3.30	22.41	0.511	0.295	6.60	6.55
With equal amount of Er	3.35	21.70	0.507	0.290	6.60	6.31
With double amount of Er	3.37	18.53	0.502	0.287	6.72	6.56

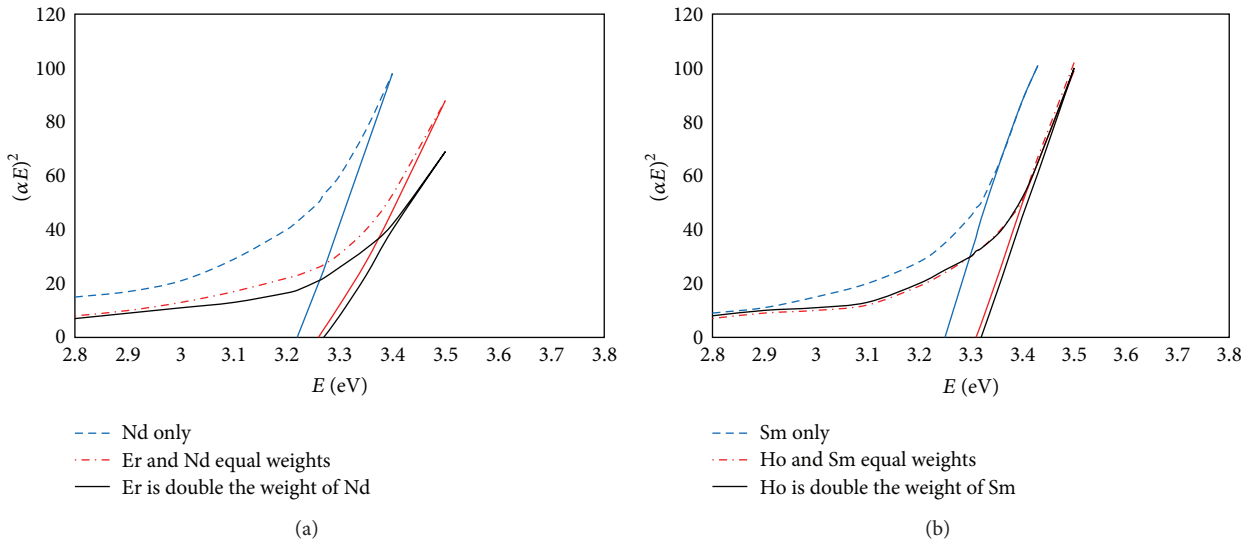

Figure 2: Direct allowed band gap calculations of ceria, doped with (a) Nd and Er and (b) Sm and Ho.

From the direct band gap calculations reported in Table 1, it can be noticed that adding Ho or Er, in addition to Nd or Sm, increases the direct allowed band gap more than the doped ceria with only Nd or Sm. This increase in the band gap becomes higher with increasing the concentration of the negative association energy elements: Ho and Er. That gives an indication that there are less Ce^{4+} ions converted to Ce^{3+} ones. In other words, these doping materials, Ho and Er, act as O-vacancies scavengers.

In the fluorescence spectroscopy, the 4 eV band gap of ceria, Ce^{4+} ions in CeO_2, is an indirect gap. Therefore, there will be a very small probability that the radiative recombination will occur when absorption takes place. At the same time, the relaxation via the 5d–4f transition of the Ce^{3+} ions in Ce_2O_3, which has a direct band gap of around 3 eV, leads to a photon emission [16, 32]. The rate at which photons are emitted from the material via spontaneous emission, which is interpreted as the peak of the emitted intensity in the power meter, is proportional to the number of excited electrons in the conduction band. Then, the more Ce^{3+} states could result in higher fluorescence emission and vice versa.

The fluorescent emissions of some examples of MDC samples are shown in Figure 3 and the complete peak emission values are reported in Table 1. The peak emission is found to be lower within mixing Ho or Er with Nd or Sm, compared to the doped ceria with only Nd or Sm, which ensures that there are less Ce^{3+} ionization states when adding the negative association lanthanide dopants. This conclusion is in good agreement with the results obtained from the direct band gap calculations.

To discuss the structural characteristics of MDC nanoparticles, examples of TEM images of these nanoparticles, associated with diffraction rings, are shown in Figure 4. The average nanoparticles' size, interplanar distances, and lattice

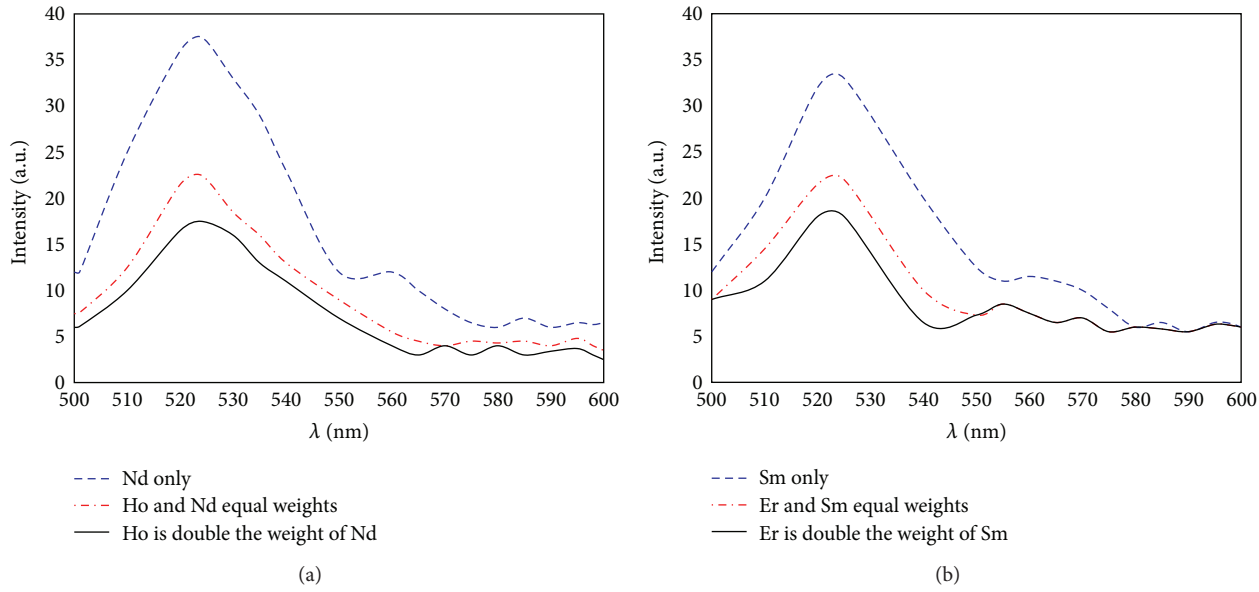

Figure 3: Fluorescence emission of ceria, doped with (a) Nd and Ho and (d) Sm and Er.

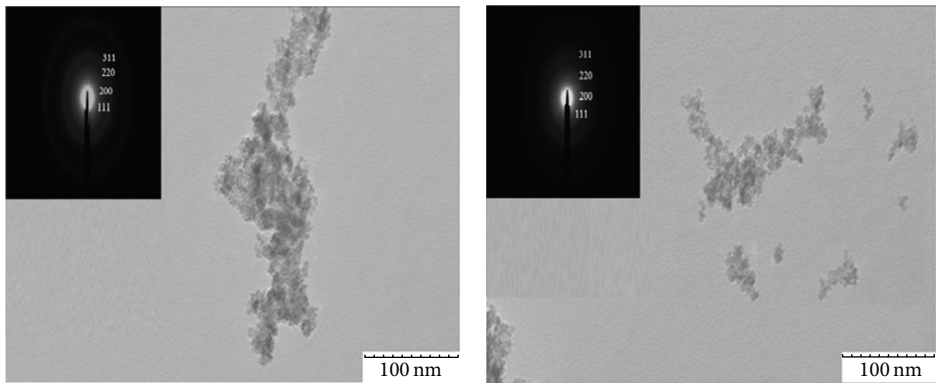

Figure 4: TEM images of some ceria nanoparticles doped with equal concentrations of (a) Nd and Ho and (b) Nd and Er.

parameters are calculated and reported in Table 1 for the whole discussed samples. From these results, it can be noticed that MDC has larger particle size, smaller interplanar distance, and lattice parameter, compared to the same characteristics obtained for ceria codoped with only positive association energy lanthanides. Lower average size and larger interplanar distance or lattice parameter in ceria nanoparticles are reported as indications for more conversion to Ce^{3+} state with forming more vacancies and vice versa.

XRD patterns of some MDC samples are presented in Figure 5. To determine the structure of the formed nanoparticles, the patterns of different samples are measured through X-ray diffractometer (XRD). From the first pattern peak, which indicates the most stable surface plane (111), among the low index planes of ceria [5], the average particles' diameter can be calculated through Scherrer's formula as follows:

$$d = \frac{0.9\lambda}{\beta \operatorname{Cos} \theta}, \quad (2)$$

where d is the average diameter of the particles, λ is the wavelength of X-ray, β is the full width half-maximum (FWHM) of the surface plane pattern, and θ is the diffraction angle. The complete results of the whole samples are reported in Table 1. These results are in good agreement with the results obtained from TEM images. Table 2 lists the results from the analysis of the doped ceria nanoparticles obtained from XPS and provides a quantitative overview of the chemical composition of each synthesized nanoparticle of doped ceria with individual positive association lanthanide and MDC samples.

4. Conclusions

Mixed doped ceria nanoparticles (MDC NPs) consist of ceria codoped with positive association energy lanthanides, such as neodymium and samarium, and negative association energy lanthanides, such as holmium and erbium. In this

Table 2: Chemical analysis of the atomic concentrations of synthesized samples using X-ray photoelectron spectroscopy (XPS).

Weight ratios	O1s	Ce3d	Nd3d	Sm3d	Ho4d	Er4d
Nd						
With no Ho or Er	66.03	10.70	0.44	0	0	0
With equal amount of Ho	62.38	12.57	1.32	0	1.24	0
With double amount of Ho	58.54	13.42	1.25	0	1.35	0
With equal amount of Er	60.51	13.51	1.14	0	0	1.01
With double amount of Er	63.75	11.25	1.24	0	0	1.57
Sm						
With no Ho or Er	65.63	12.14	0	1.09	0	0
With equal amount of Ho	62.37	15.07	0	1.14	0.94	0
With double amount of Ho	59.77	12.24	0	0.8	1.46	0
With equal amount of Er	61.58	13.87	0	1.26	0	0.96
With double amount of Er	61.48	13.79	0	1.19	0	2.01

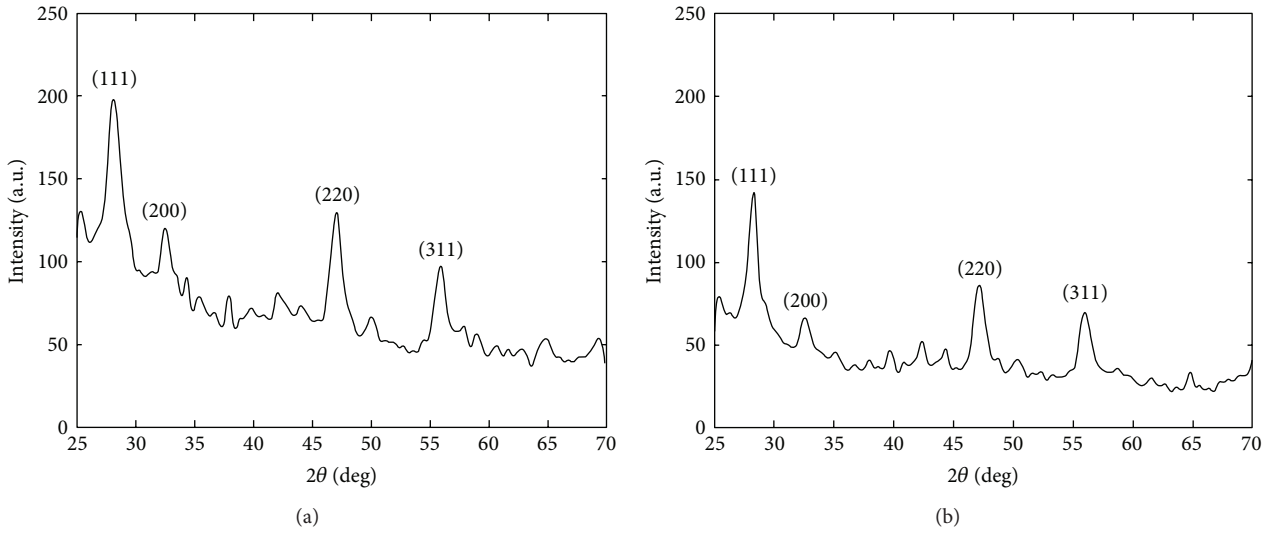

Figure 5: XRD pattern of some ceria nanoparticles doped with equal concentrations of (a) Nd and Ho and (b) Sm and Er.

work, it is proved that the Ce^{3+} ionization state in MDC could be reduced compared to ceria doped with only positive association lanthanides. The consistency of this conclusion is verified through four different optical and structural characteristics. Adding these negative association lanthanides to the doped ceria, with positive association dopants, increases the direct band gap, decreases the emitted peak fluorescent intensity, increases the average size of the nanoparticles, and decreases the lattice parameter compared to doped ceria with only positive association lanthanides. The last two structural measurements are verified from TEM images and the average particles' size that is calculated from the XRD pattern, which agrees with the average size found from TEM. In summary, this work investigates, with different experimental procedures, a novel conclusion that the negative association lanthanide dopants can act as oxygen vacancies scavengers in ceria nanoparticles. The control of these defects through the suggested doping technique can lead to a promising impact on many applications in electronic devices, gas sensing, and biomedical applications.

Conflict of Interests

The authors declare that there is no conflict of interests regarding the publication of this paper.

Acknowledgments

This work was funded in part by a NSF STTR Phase I grant with MW Photonics (award 0930364). The first author, Dr. Shehata, is supported by a fund through Virginia Tech Middle East and North Africa (VT-MENA) Program. The authors thank Dr. Niven Monsegue, Dr. Jerry Hunter, and Andrew Giordani from the Nanotechnology Characterization and Fabrication Laboratory, Institute of Critical Technologies and Applied Science at Virginia Tech, for their training and assistance with the TEM and XPS measurements. Also, the authors appreciate the support of Mr. Don Leber, Manager of the Micron Technology Semiconductor Processing Laboratory at Virginia Tech.

References

[1] S. Tsunekawa, T. Fukuda, and A. Kasuya, "Blue shift in ultraviolet absorption spectra of monodisperse CeO_{2-x} nanoparticles," *Journal of Applied Physics*, vol. 87, no. 3, pp. 1318–1321, 2000.

[2] M. Oh, J. Nho, S. Cho, J. Lee, and R. Singh, "Polishing behaviors of ceria abrasives on silicon dioxide and silicon nitride CMP," *Powder Technology*, vol. 206, no. 3, pp. 239–245, 2011.

[3] M. Das, S. Patil, N. Bhargava et al., "Auto-catalytic ceria nanoparticles offer neuroprotection to adult rat spinal cord neurons," *Biomaterials*, vol. 28, no. 10, pp. 1918–1925, 2007.

[4] B. C. Steele and A. Heinzel, "Materials for fuel-cell technologies," *Nature*, vol. 414, no. 6861, pp. 345–352, 2001.

[5] S. Deshpande, S. Patil, S. Kuchibhatla, and S. Seal, "Size dependency variation in lattice parameter andvalency states in nanocrystalline cerium oxide," *Applied Physics Letters*, vol. 87, no. 13, pp. 133113/1–133113/3, 2005.

[6] R. Gerhardt, W.-K. Lee, and A. S. Nowick, "Anelastic and dielectric relaxation of scandia-doped ceria," *Journal of Physics and Chemistry of Solids*, vol. 48, no. 6, pp. 563–569, 1987.

[7] E. Suda, B. Pacaud, and M. Mori, "Sintering characteristics, electrical conductivity and thermal properties of La-doped ceria powders," *Journal of Alloys and Compounds*, vol. 408–412, pp. 1161–1164, 2006.

[8] S. Dikmen, P. Shuk, and M. Greenblatt, "Hydrothermal synthesis and properties of $Ce_{1-x}La_xO_{2-\delta}$ solid solutions," *Solid State Ionics*, vol. 126, no. 1-2, pp. 89–95, 1999.

[9] H. Yamamura, S. Takeda, and K. Kakinuma, "Dielectric relaxations in the $Ce_{1-x}Nd_xO_{2-\delta}$ system," *Solid State Ionics*, vol. 178, no. 15–18, pp. 1059–1064, 2007.

[10] T. Dhannia, S. Jayalekshmi, M. C. Santhosh Kumar, T. Prasada Rao, and A. Chandra Bose, "Effect of aluminium doping and annealing on structural and optical properties of cerium oxide nanocrystals," *Journal of Physics and Chemistry of Solids*, vol. 70, no. 11, pp. 1443–1447, 2009.

[11] D. Andersson, S. Simak, N. Skorodumova, I. Abrikosov, and B. Johansson, "Optimization of ionic conductivity in doped ceria," *Proceedings of the National Academy of Sciences of the United States of America*, vol. 103, no. 10, pp. 3518–3521, 2006.

[12] X. Wei, W. Pan, L. Cheng, and B. Li, "Atomistic calculation of association energy in doped ceria," *Solid State Ionics*, vol. 180, no. 1, pp. 13–17, 2009.

[13] M. Nakayama and M. Martin, "First-principles study on defect chemistry and migration of oxide ions in ceria doped with rare-earth cations," *Physical Chemistry Chemical Physics*, vol. 11, pp. 3241–3249, 2009.

[14] F. Zhang, P. Wang, J. Koberstein, S. Khalid, and S.-W. Chan, "Cerium oxidation state in ceria nanoparticles studied with X-ray photoelectron spectroscopy and absorption near edge spectroscopy," *Surface Science*, vol. 563, no. 1–3, pp. 74–82, 2004.

[15] D. R. Mullins, S. H. Overbury, and D. R. Huntley, "Electron spectroscopy of single crystal and polycrystalline cerium oxide surfaces," *Surface Science*, vol. 409, no. 2, pp. 307–319, 1998.

[16] L. Qiu, F. Liu, L. Zhao, Y. Ma, and J. Ya, "Comparative XPS study of surface reduction for nanocrystalline and microcrystalline ceria powder," *Applied Surface Science*, vol. 252, no. 14, pp. 4931–4935, 2006.

[17] F. El-Diasty, "Coherent anti-Stokes Raman scattering: spectroscopy and microscopy," *Vibrational Spectroscopy*, vol. 55, pp. 1–37, 2011.

[18] C. O. Chui, H. Kim, P. C. McIntyre, and K. C. Saraswat, "Atomic layer deposition of high-κ dielectric for germanium MOS applications—substrate surface preparation," *IEEE Electron Device Letters*, vol. 25, no. 5, pp. 274–276, 2004.

[19] N. Shehata, K. Meehan, and D. Leber, "Study of fluorescence quenching in aluminum-doped ceria nanoparticles: potential molecular probe for dissolved oxygen," *Journal of Fluorescence*, vol. 23, no. 3, pp. 527–532, 2013.

[20] S. Babu, A. Velez, K. Wozniak, J. Szydlowska, and S. Seal, "Electron paramagnetic study on radical scavenging properties of ceria nanoparticles," *Chemical Physics Letters*, vol. 442, no. 4–6, pp. 405–408, 2007.

[21] H. Chen and H. Chang, "Homogeneous precipitation of cerium dioxide nanoparticles in alcohol/water mixed solvents," *Colloids and Surfaces A: Physicochemical and Engineering Aspects*, vol. 242, pp. 61–69, 2004.

[22] N. Shehata, K. Meehan, M. Hudait, and N. Jain, "Control of oxygen vacancies and Ce^{+3} concentrations in doped ceria nanoparticles via the selection of lanthanide element," *Journal of Nanoparticle Research*, vol. 14, pp. 1173–1183, 2012.

[23] N. Shehata, K. Meehan, I. Hassounah et al., "Reduced erbium-doped ceria nanoparticles: one nano-host applicable for simultaneous optical down- and up-conversions," *Nanoscale Research Letters*, vol. 9, no. 1, p. 231, 2014.

[24] N. J. Lawrence, K. Jiang, and C. L. Cheung, "Formation of a porous cerium oxide membrane by anodization," *Chemical Communications*, vol. 47, no. 9, pp. 2703–2705, 2011.

[25] A. Trovarelli, *Catalysis by Ceria and Related Materials*, Imperial College Press, 2005.

[26] S. Basu, P. S. Devi, and H. S. Maiti, "Synthesis and properties of nanocrystalline ceria powders," *Journal of Materials Research*, vol. 19, no. 11, pp. 3162–3171, 2004.

[27] H. Guo, "Green and red upconversion luminescence in CeO_2:Er^{3+} powders produced by 785 nm laser," *Journal of Solid State Chemistry*, vol. 180, no. 1, pp. 127–131, 2007.

[28] L. Qiu, F. Liu, L. Zhao, Y. Ma, and J. Yao, "Comparative XPS study of surface reduction for nanocrystalline and microcrystalline ceria powder," *Applied Surface Science*, vol. 25, no. 14, pp. 4931–4935, 2006.

[29] J. Pankove, *Optical Processes in Semiconductors*, Dover Publications, New York, NY, USA, 1971.

[30] P. Patsalas, S. Logothetidis, L. Sygellou, and S. Kennou, "Structure-dependent electronic properties of nanocrystalline cerium oxide films," *Physical Review B*, vol. 68, no. 3, Article ID 035104, 2003.

[31] L. Yin, Y. Wang, G. Pang, Y. Koltypin, and A. Gedanken, "Sonochemical synthesis of cerium oxide nanoparticles—effect of additives and quantum size effect," *Journal of Colloid and Interface Science*, vol. 246, no. 1, pp. 78–84, 2002.

[32] N. Shehata, K. Meehan, I. Ashry, I. Kandas, and Y. Xu, "Lanthanide-doped ceria nanoparticles as fluorescence-quenching probes for dissolved oxygen," *Sensors and Actuators B: Chemical*, vol. 183, pp. 179–186, 2013.

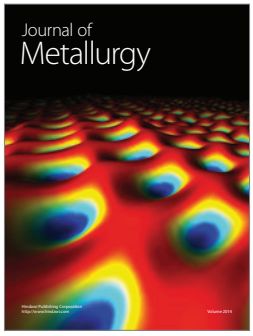

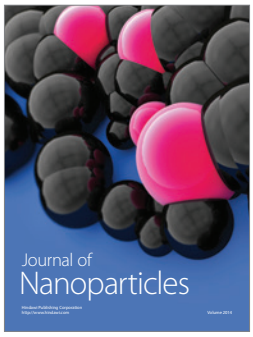

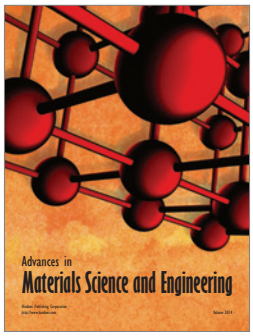

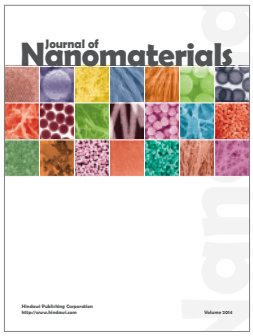

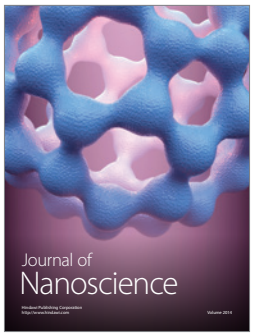

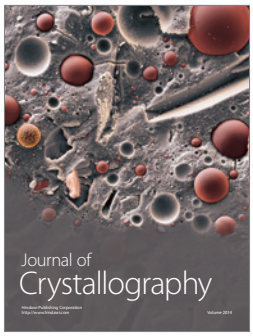

Hindawi

Submit your manuscripts at
http://www.hindawi.com